CrossMark
click for updates



# AMCase is a crucial regulator of type 2 immune responses to inhaled house dust mites

Lark Kyun Kim[a], Rimpei Morita[a,1], Yasushi Kobayashi[a], Stephanie C. Eisenbarth[a,b], Chun Geun Lee[c,2], Jack Elias[c,2], Elizabeth E. Eynon[a], and Richard A. Flavell[a,d,3]

[a]Department of Immunobiology, [b]Department of Laboratory Medicine, [c]Section of Pulmonary and Critical Care Medicine, and [d]Howard Hughes Medical Institute, Yale University School of Medicine, New Haven, CT 06520

Contributed by Richard A. Flavell, April 21, 2015 (sent for review December 8, 2014; reviewed by Neil A. R. Gow and Myung Hyun Sohn)

**Chitinases are enzymes that cleave chitin, a component of the exoskeleton of many organisms including the house dust mite (HDM). Here we show that knockin mice expressing an enzymatically inactive acidic mammalian chitinase (AMCase), the dominant true chitinase in mouse lung, showed enhanced type 2 immune responses to inhaled HDM. We found that uncleaved chitin promoted the release of IL-33, whereas cleaved chitin could be phagocytosed and could induce the activation of caspase-1 and subsequent activation of caspase-7; this results in the resolution of type 2 immune responses, probably by promoting the inactivation of IL-33. These data suggest that AMCase is a crucial regulator of type 2 immune responses to inhaled chitin-containing aeroallergens.**

AMCase | chitin | house dust mite | IL-33

Allergic asthma, affecting millions of people worldwide, is a disease characterized by chronic airway inflammation (1–3). It is well established that immune responses to inhaled allergens like house dust mite (HDM), cockroach, and animal dander provide much of the underlying basis of asthma pathogenesis such as eosinophilic inflammation of the airway, goblet cell metaplasia, and bronchial hyperreactivity (1–5). HDM is one of the commonest allergens, and up to 85% of asthmatics are known to be typically HDM-allergic (1). The allergic potential of HDM relies on the mites themselves and their fecal pellets (1).

Chitin, a long chain polymer of an *N*-acetylglucosamine, is the second most abundant polysaccharide in nature after cellulose (6, 7). It functions as a major structural polymer in many lower life forms including the cell walls of bacteria and fungi, the shell of crabs and shrimp, the exoskeleton of HDM and cockroaches, and the microfilarial sheath of parasitic nematodes (6, 7). It is not expressed by mammals (6, 7). Several lines of evidence indicate that chitin can act as an immune stimulator (7). First, it has been reported that i.v. administration of size-fractionated (i.e., small) chitin particles induced the production of interleukin-12 (IL-12), TNFα, and IL-18 from macrophages and the production of IFN-γ from natural killer cells (components common to a Th1-type response) (7, 8). In addition, it has been demonstrated that chitin could inhibit type 2 immunity including IgE production and eosinophilia (7, 9). Similarly, it has been demonstrated that intranasal administration of chitin microparticles down-regulated allergic hypersensitivity to HDM (7, 10). However, in contrast to the above-mentioned studies, it has been reported that intranasal administration of chitin beads into mice induced the accumulation of IL-4–expressing innate immune cells including eosinophils and basophils and also induced alternatively activated macrophages (11). Thus, chitin obviously plays a role as a stimulator and/or a regulator of immune responses although the exact role of chitin is controversial.

Chitinases are enzymes that degrade chitin and are made both by organisms that express chitin, including parasites, and by the hosts that harbor these organisms (7). Mammals, including humans, do not synthesize chitin but all mammals studied encode chitinases (7). Among the several chitinases, there are only two true chitinases having chitolytic enzyme activity that breaks down glycosidic bonds of chitin in humans and mice; these are chitotriosidase and acidic mammalian chitinase (AMCase) (7). Although chitotriosidase is expressed in both humans and mice, it is expressed at low levels in mouse lung, and thus AMCase is believed to be the dominant true chitinase in mouse lung (12–14). Expression of AMCase has been shown to be increased in human asthma patients and is also induced in mice in an aeroallergen asthma model (15). In nonchitin-dependent asthma models such as the ovalbumin-induced asthma model and IL-13–overexpressing transgenic mice (15), blocking of AMCase by neutralizing antibody ameliorated type 2 inflammation and airway hyperreactiveness. However, in the chitin-beads model described above, chitin beads pretreated with recombinant AMCase failed to induce type 2 immune responses, and also chitin beads did not induce immune responses in AMCase–overexpressing transgenic mice (11).

Chitinase-related proteins, other than chitotriosidase and AMCase in humans and mice, can bind chitin but lack chitinase activity as a result of mutations in the otherwise highly conserved putative enzyme active sites; they are therefore called chitinase-like proteins (CLPs) (7, 16). Breast regression protein 39 (BRP-39) and its human homolog YKL-40 are CLPs induced in the aeroallergen asthma mouse model and human asthma patients, respectively (7, 17). In KO mice in which BRP-39 was deleted, type 2 immune responses were diminished in the OVA-induced mouse model or IL-13–overexpressing transgenic mice, but the immune responses were rescued by crossing with an

## Significance

**Millions of people are affected by asthma and that number is growing. A clear understanding of how the disease develops is lacking. The immune responses to inhaled allergens like house dust mite (HDM) provide much of the basis of asthma. Acidic mammalian chitinase (AMCase) is an enzyme that degrades chitin, a major structural polymer in the exoskeleton of HDM. By the use of a newly generated enzymatically dead AMCase knockin mouse, we found that AMCase enzymatic activity is of critical importance in the control of type 2 immune responses to inhaled HDM. This discovery may help the understanding of the mechanisms that govern the development of chitin-related asthma and allergy and may lead to new therapeutic strategies in these disorders.**

Author contributions: R.A.F. directed the project; L.K.K., E.E.E., and R.A.F. designed research; L.K.K., R.M., and Y.K. performed research; S.C.E., C.G.L., and J.E. analyzed data; and L.K.K., E.E.E., and R.A.F. wrote the paper.

Reviewers: N.A.R.G., University of Aberdeen; and M.H.S., Yonsei University College of Medicine.

The authors declare no conflict of interest.

[1]Present address: Department of Microbiology and Immunology, Keio University School of Medicine, Tokyo 160-8582, Japan.

[2]Present address: Department of Molecular Microbiology and Immunology, Brown University, Providence, Rhode Island 02912.

[3]To whom correspondence should be addressed. Email: richard.flavell@yale.edu.

This article contains supporting information online at www.pnas.org/lookup/suppl/doi:10.1073/pnas.1507393112/-/DCSupplemental.

YKL-40–overexpressing transgenic mouse (17). However, the roles in immune responses of many other CLPs are still largely unknown.

Taken together, despite a number of reports demonstrating a crucial role of chitin and chitinase (and CLPs) in immune responses, their exact function seems to be controversial. More specifically, a clear distinction of the functional roles of merely binding chitin as mediated by the CLPs versus cleaving chitin as performed by chitotriosidase and AMCase has not been achieved. Moreover, most studies have been done in a chitin-independent aeroallergen mouse model such as the OVA-induced model or IL-13–overexpressing transgenic mice. In our present study, we generated enzymatically deficient *AMCase* knockin (*AMCase-ED*) mice, which consequently resulted in the expression of inactive chitinase that is still able to bind to chitin. After intranasal administration of HDM extracts into mice, we found that *AMCase-ED* mice showed enhanced type 2 immune responses. Unlike cleaved chitin, the chitin that was not cleaved by enzymatic dead AMCase in the lung failed to be phagocytosed, which led to accumulation of IL-33, and thus prolonged exposure of the lungs to this cytokine concomitantly enhanced type 2 immune responses. In contrast, in the wild-type mice, the chitin that was adequately cleaved by active AMCase was phagocytosed, which led to cleavage and inactivation of IL-33 and resolution of type 2 immune responses via caspase-1 and caspase-7 cascades.

## Results

***AMCase-ED* Mice Show Enhanced Type 2 Immune Responses to Inhaled HDM.** To investigate the function of enzymatic activity of AMCase in airway inflammation, we made an enzymatically defective *AMCase-ED* mouse by replacing the aspartic acid with alanine in the catalytic domain of AMCase (Fig. 1*A* and Fig. S1). It has been previously shown, by transfecting the designed construct into a cell line and measuring chitinase activity, that this mutation of AMCase rendered the enzyme inactive without affecting the binding of AMCase to chitin (18). These mice have no overt developmental or phenotypic defects and are born at normal Mendelian ratios. To induce type 2 immune responses, we decided to use HDM because, as one of the common allergens, HDM is a very pathologically relevant agent (1). First, we wanted to determine the levels of chitin in HDM (Greer Laboratories). Although it is clear that HDM contains chitin, the commercial preparations widely used in many previous HDM studies were prepared as extracts after filtration, suggesting that larger fragments of chitin may have been removed. We compared purified chitin with the purchased HDM and confirmed that all batches of HDM used in this study contained chitin (Fig. S2*A*). We then treated wild-type mice intranasally with HDM and unfiltered raw HDM that contains larger fragments of chitin (Greer Laboratories). We counted total cell number in the bronchoalveolar lavage, which was increased following administration of HDM compared with administration of control PBS (Fig. 1*B* and Fig. S2*B*). Interestingly, *AMCase-ED* mice showed a greater increase in cell number, consisting mostly of eosinophils in the BAL after HDM administration. Similarly, raw HDM treatment induced a greater increase in cell number compared with HDM treatment, suggesting that the amount of chitin or the size of the chitin plays a major role in cellular infiltration in the BAL. However, after administration of raw HDM, *AMCase-ED* mice did not show clear differences compared with control mice as much as after administration of HDM, suggesting that increased amounts of the larger fragments of chitin in raw HDM may lead to accumulation of excessive levels of substrate that WT mice cannot cleave and therefore result in the lack of significant differences between WT and *AMCase-ED* mice. Heat treatment of either HDM or raw HDM did not significantly affect lung infiltrates, although HDM heat treatment showed a reduced trend, implying the roles of heat-insensitive chitin and

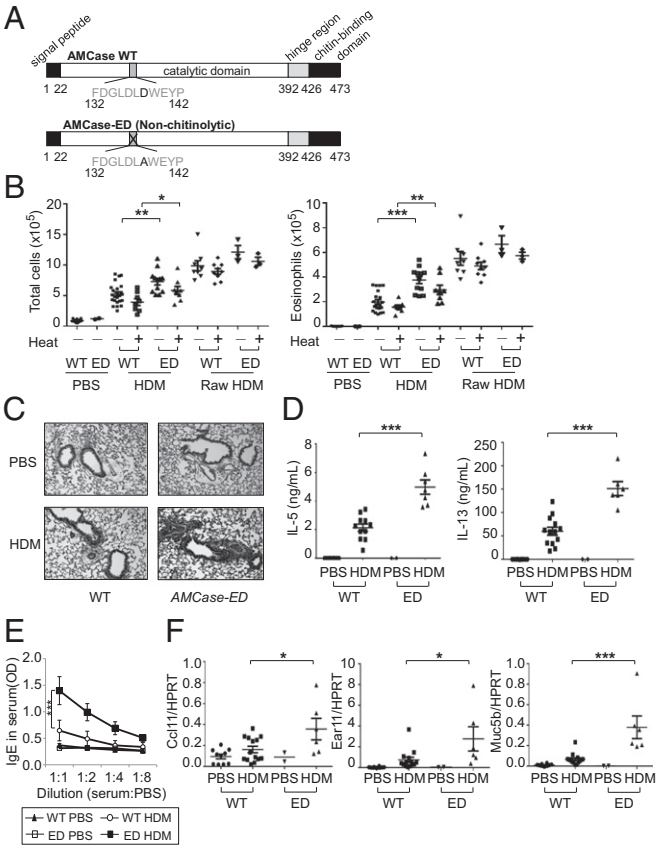


**Fig. 1.** Enhanced type 2 immune responses to inhaled HDM in *AMCase-ED* mice. (*A*) The schematic domains of AMCase. Aspartic acid is replaced with alanine in active site of catalytic domain of AMCase in *AMCase-ED* mice. (*B*) The number of total cells (*Left*) or eosinophils (*Right*) in the BAL of WT or *AMCase-ED* mice after administration of PBS, HDM, or raw HDM with (+) or without (–) pretreatment at 95 °C for 10 min. (*C*) H&E staining of lung sections of WT or *AMCase-ED* mice after administration of PBS or HDM (magnification: 20x). (*D*) The production of IL-5 (*Left*) and IL-13 (*Right*). The cells of lung-draining lymph nodes from WT or *AMCase-ED* mice after administration of PBS or HDM were restimulated in vitro with HDM and mitomycin-C–treated splenocytes for 48 h. Supernatants were collected and analyzed for IL-5 and IL-13 by ELISA. (*E*) The level of IgE in serum of WT or *AMCase-ED* mice after administration of PBS or HDM. The serum was diluted with PBS sequentially and analyzed for IgE by ELISA. (*F*) The expression of ccl11, ear11, and muc5b, normalized to hypoxanthine-guanine phosphoribosyltransferase, in the lung of WT or *AMCase-ED* mice after administration of PBS or HDM. $*P < 0.05$, $**P < 0.01$, and $***P < 0.001$, unpaired Student's *t* test. Data were combined from at least four independent experiments. Error bars indicate the SEM.

other carbohydrates. There were no significant differences in other cell types (Fig. S2*B*). We decided to use commercially prepared filtered HDM (hereafter referred to as HDM) for most experiments. Next we checked the expression of AMCase in lung (Fig. S2*C*). Mice that were administrated HDM showed elevated expression of AMCase compared to PBS-treated control mice, but there was no difference in AMCase expression between WT mice and *AMCase-ED* mice after HDM administration. However, although chitinase activity was also elevated after HDM administration compared with PBS-treated control mice, there was no elevation of chitinase activity in *AMCase-ED* mice, confirming that *AMCase-ED* mice lack most chitinase activity and that AMCase is a major contributor to the chitinase activity in this tissue under these conditions (Fig. S2*D*). The expression of other CLPs such as Brp39, Ym1, and Ym2 was also increased after HDM administration (Fig. S2*E*), but the

expression of chitotriosidase, which is the only other active chitinase, was not detected even after HDM administration. Histologic examination also showed more severe inflammation in *AMCase-ED* mice after HDM administration (Fig. 1*C*). To measure the expression of IL-5 and IL-13, T cells were collected from draining lymph nodes and then restimulated with HDM. T cells from HDM-administered *AMCase-ED* mice showed more IL-5 and IL-13 production compared with T cells from HDM-administrated control mice (Fig. 1*D*). Total serum IgE levels and also HDM-specific IgE levels were higher in HDM-administrated *AMCase-ED* mice (Fig. 1*E* and Fig. S2*F*), and, finally, the expression of the chemokines ccl11 and ear11 and the mucin gene *muc5b* was also increased in the lung from HDM-administrated *AMCase-ED* mice (Fig. 1*F*). Altogether, these results indicated that there is a greater type 2 immune response in *AMCase-ED* mice in response to inhaled HDM than in mice with intact AMCase activity.

**Uncleaved Chitin Promotes Stronger Type 2 Immune Responses.** To check whether the enhanced immune response to inhaled HDM in *AMCase-ED* mice is due to chitin and also due to the lack of chitinase activity in *AMCase-ED* mice, we directly administered chitin intranasally to these mice. For this study, we fractionated purified chitin by size and then separated the chitin into three size bins: small (less than 40 μm), intermediate (40–70 μm), and large (70–100 μm) chitin (Fig. 2*A*). We found that the expression of AMCase transcript was increased in mice that received small chitin compared to PBS-treated control mice (Fig. 2*B*). Large chitin-treated mice showed still greater expression of AMCase compared with small chitin-administrated mice. Other CLPs such as Brp39, Ym1, and Ym2 were also induced after chitin administration and expressed at higher levels after administration of large chitin rather than small chitin (Fig. S3*A*). There was no difference in AMCase expression between WT and *AMCase-ED* mice after small- or large-chitin administration (Fig. 2*B*). Infiltration of immune cells into the lungs was greater upon administration of large versus small chitin to mice, and the majority of cells that were increased were eosinophils (Fig. 2*C*). Histologic analysis also showed more severe inflammation following administration of large rather than small chitin (Fig. 2*D*). *AMCase-ED* mice showed greater cellular infiltration in the BAL compared with WT mice upon administration of either small or large chitin (Fig. 2*E* and Fig. S3*B*). The expression levels of ccl11, ear11 and muc5b was greater following administration of large chitin versus small chitin and their expression was also induced to a higher level in *AMCase-ED* mice comparing to WT mice (Fig. 2*F*). We therefore concluded that chitin itself could elicit pulmonary inflammation and that uncleaved chitin causes a stronger response than cleaved chitin. Moreover, we observed that the responses of *AMCase-ED* mice were stronger in all parameters measured, probably due to a failure to cleave chitin.

**Chitin Uncleaved by Enzymatically Dead AMCase Is Not Phagocytosed and Fails to Activate Caspase-1.** Chitosan, a commercially available deacetylated chitin, but not chitin, has been reported to activate caspase-1 by the phagocytic pathway (19). It has also been shown that the size of chitosan was important for phagocytosis (19, 20). In fact, the differential role of the size of chitin was supported by another report (21). In our system, chitosan indeed seemed to induce more IL-1β production than chitin in vitro, probably due to the easier accessibility of chitosan to the cells, which might derive from the different solubility between chitin and chitosan, but chitin itself also significantly induced IL-1β (Fig. S4*A* and Fig. 3*C*). As chitin is the second most abundant polysaccharide in nature and a true component of the exoskeleton of HDM (1, 7), we reasoned that chitin would be a more physiologically relevant inducer, and thus we decided to use chitin in our experiments to examine the role of the enzymatic activity of AMCase. Although we purified the chitin to reduce endotoxin, we still could not

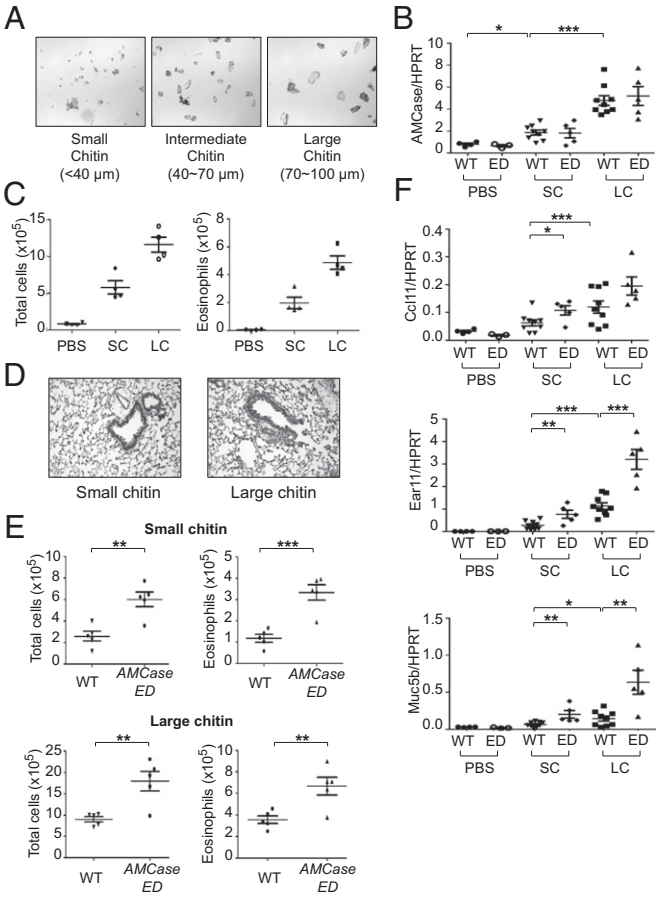


**Fig. 2.** The enhanced type 2 immune responses to inhaled chitin in *AMCase-ED* mice. (*A*) The images of fractionated chitin. (*B*) The expression of AMCase, normalized to HPRT, in the lung of WT or *AMCase-ED* mice after administration of PBS, small-chitin, or large-chitin fragments. (*C*) The number of total cells (*Left*) or eosinophils (*Right*) in the BAL of WT mice after administration of PBS, small-chitin, or large-chitin fragments. (*D*) H&E staining of lung sections of WT mice after administration of small-chitin or large-chitin fragments (magnification: 20x). (*E*) The number of total cells and eosinophils in the BAL of WT mice after administration of small-chitin (*Top*) and large-chitin fragments (*Bottom*). (*F*) The expression of ccl11, ear11, and muc5b, normalized to HPRT in the lung of WT or *AMCase-ED* mice after administration of PBS, small-chitin, or large-chitin fragments. $*P < 0.05$, $**P < 0.01$, and $***P < 0.001$, unpaired Student's *t* test. Data were combined from at least three independent experiments. Error bars indicate the SEM.

exclude the possibility of contamination of these preparations with small amounts of endotoxin or other contaminants (Fig. S4*B*). To focus on the effect of chitin and eliminate the potent effects of contaminating endotoxin, we pretreated the macrophages with LPS, so that incremental effects of small amounts of LPS derived from the chitin would be negligible, and actually we did not see a significant difference between priming with and without LPS. First, we took peritoneal macrophages from WT and *AMCase-ED* mice, as AMCase is secreted from both macrophages and lung epithelial cells. Peritoneal macrophages were treated with a chitin mixture (less than 70 μm) and then assayed for chitinase activity (Fig. 3*A*). We found that chitinase activity was induced, peaked at 2 h after chitin treatment, and was sustained for 4 h. Chitin-treated macrophages showed caspase-1 activation in a dose-dependent manner, whereas, interestingly, caspase-1 activation in the macrophages from *AMCase-ED* mice was dramatically diminished (Fig. 3*B*). Again, we cannot exclude the possibility that the residual endotoxin contamination in our chitin preparation favors caspase-1 activation. Regarding

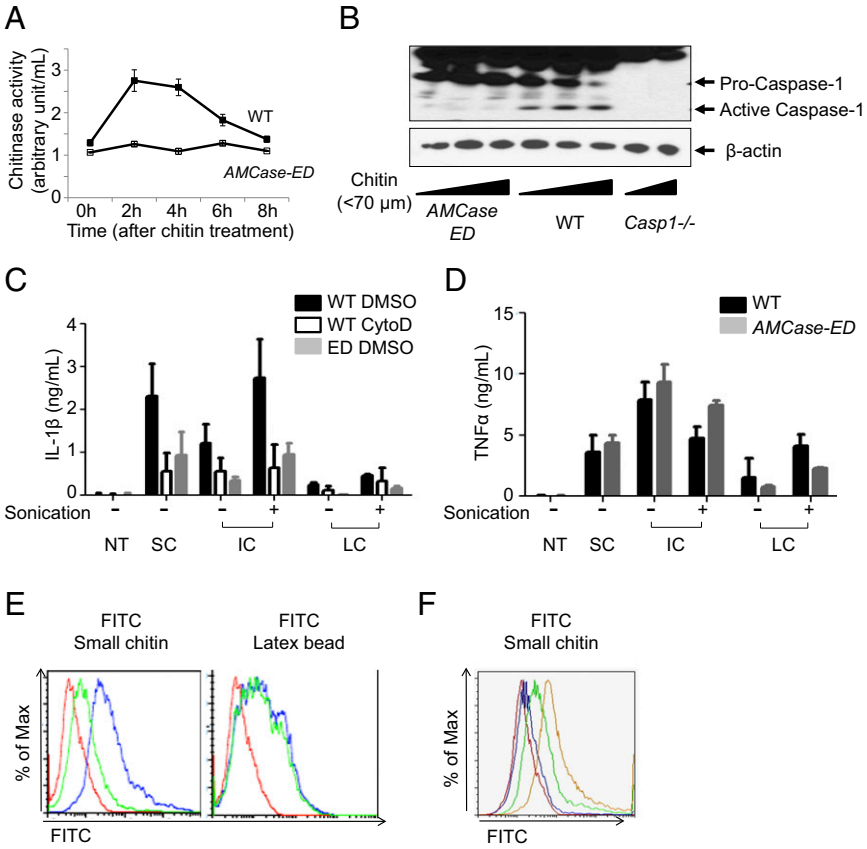


**Fig. 3.** Defective caspase-1 activation after administration of chitin in *AMCase-ED* cells. (*A*) Chitinase activity in the supernatants of LPS-primed peritoneal macrophages from WT or *AMCase-ED* mice after chitin mixture (less than 70 μm) treatments. (*B*) Immunoblot analysis of caspase-1 and β-actin in LPS-primed peritoneal macrophages from WT, *AMCase-ED*, or *Casp1*$^{-/-}$ mice. (*C*) Production of IL-1β in the supernatants of LPS-primed peritoneal macrophages from WT or *AMCase-ED* mice with pretreatment of DMSO or cytochalasin D after treatment of small, intermediate, or large-chitin fragments with (+) or without (–) sonication. (*D*) Production of TNFα in the supernatants of LPS-primed peritoneal macrophages from WT or *AMCase-ED* mice after treatment of small-, intermediate-, or large-chitin fragments with (+) or without (–) sonication. (*E*) Histograms of fluorescence distribution of the peritoneal macrophages from WT (blue) or *AMCase-ED* mice (green) after FITC-conjugated small-chitin (*Left*) or latex bead (*Right*) treatment. Red represents WT cells without any treatment. (*F*) Histograms of fluorescence distribution of the mixture of peritoneal macrophages from WT and *AMCase-ED* mice. Yellow represents 100% of WT cells, green represents the mixture of 66% of WT cells and 33% of *AMCase-ED* cells, and blue represents the mixture of 33% of WT cells and 66% of *AMCase-ED* cells after FITC-conjugated small-chitin fragment treatment. Red represents the mixture of 50% of WT cells and 50% of *AMCase-ED* cells without any treatment. Data are representative of at least three independent experiments. Error bars indicate the SD.

the production of IL-1β and TNFα, their expression showed dose- and time-dependent induction (Fig. S4*A*). As reported previously (19), small chitin induced greater production of IL-1β rather than intermediate or large chitin, and we also confirmed that intermediate chitin fragmented by sonication could induce IL-1β to a greater extent than untreated intermediate chitin (Fig. 3*C*). The production of IL-1β was reduced in cytochalasin D pretreated macrophages, suggesting that IL-1β production by chitin is dependent on phagocytosis as described in a previous report (19). Interestingly, the production of IL-1β was reduced in macrophages from *AMCase-ED* mice upon the treatment of all sizes of chitin fragments whereas the production of TNFα was unaltered (Fig. 3*D*). To further investigate whether the reduced production of IL-1β from *AMCase-ED* macrophages is due to a defect in phagocytosis, we labeled small chitin with FITC and then analyzed the cells by flow cytometry (Fig. 3*E*). The macrophages from WT mice took up FITC-labeled chitin to a greater extent than the macrophages from *AMCase-ED* mice, but their ability to phagocytose similar amounts of FITC-labeled latex beads suggests that the deficient chitin uptake in macrophages from *AMCase-ED* mice was due to the inability to cleave chitin because of the enzymatically dead AMCase, rather than due to a fundamental problem with phagocytosis itself. We also confirmed that the phagocytic efficiency was dependent on the amounts of active AMCase from WT macrophages as, when we mixed the cells from WT and *AMCase-ED* mice, the WT enzyme complemented the deficiency in the *AMCase-ED* cells (Fig. 3*F*). Moreover, we found that phagocytosis of chitin was blocked by AMCase inhibitor (bisdionin F) (Fig. S4*C*). Taken together, we concluded that cleaved chitin was phagocytosed, leading to the activation of caspase-1 and the production of IL-1β, whereas uncleaved chitin was not phagocytosed and was associated with reduced activation of both caspase-1 and the production of IL-1β.

***Casp1*$^{-/-}$ Mice Show Enhanced Type 2 Immune Responses After HDM Treatment.** The above-mentioned results predicted a role for caspase-1 in the airway response to chitin, and thus for HDM. We therefore examined the immune responses of *Casp1*$^{-/-}$ mice after HDM administration. *Casp1*$^{-/-}$ mice showed a greater cell infiltration in the BAL, and the majority of the increased cells were eosinophils (Fig. 4*A* and Fig. S5*A*). Histologic analysis also revealed greater inflammation in *Casp1*$^{-/-}$ mice (Fig. 4*B*), and the levels of both IL-5 and IL-13 from T cells from draining lymph nodes of *Casp1*$^{-/-}$ mice were elevated compared with wild-type mice when we restimulated them with HDM (Fig. 4*C*). Moreover, both total IgE levels and HDM-specific IgE levels

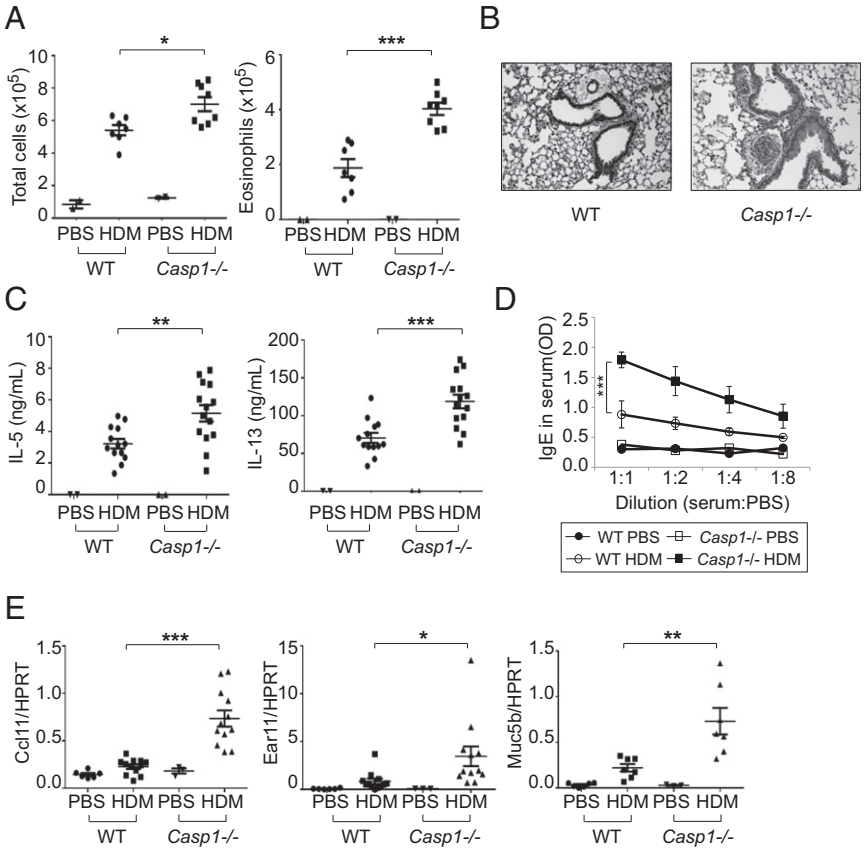


**Fig. 4.** Enhanced type 2 immune responses to inhaled HDM in *Casp1*$^{-/-}$ mice. (*A*) The number of total cells (*Left*) and eosinophils (*Right*) in the BAL of WT or *Casp1*$^{-/-}$ mice after administration of HDM. (*B*) H&E staining of lung sections of WT or *Casp1*$^{-/-}$ mice after administration of HDM (magnification: 20x). (*C*) Production of IL-5 (*Left*) and IL-13 (*Right*). The cells of lung-draining lymph nodes from WT or *Casp1*$^{-/-}$ mice after administration of HDM were restimulated in vitro with HDM and mitomycin-C–treated splenocytes for 48 h. Supernatants were collected and analyzed for IL-5 and IL-13 by ELISA. (*D*) Levels of IgE in serum of WT or *Casp1*$^{-/-}$ mice after administration of HDM. The serum was diluted with PBS sequentially and analyzed for IgE by ELISA. (*E*) Expression of ccl11, ear11, and muc5b, normalized to HPRT, in the lung of WT or *Casp1*$^{-/-}$ mice after administration of PBS or HDM. $^{*}P < 0.05$, $^{**}P < 0.01$, and $^{***}P < 0.001$, unpaired Student's *t* test. Data were combined from at least three independent experiments. Error bars indicate the SEM.



were indeed higher in *Casp1*$^{-/-}$ mice (Fig. 4*D* and Fig. S5*B*), and ccl11, ear11, and muc5b were expressed at a higher level in the lungs of *Casp1*$^{-/-}$ mice (Fig. 4*E*). These results are in contrast to previous reports showing less inflammation in *Casp1*$^{-/-}$ mice after OVA administration (22) and increased levels of IL-1β in asthma patients (23–25). However, the OVA model is chitin-independent so we inferred that chitin was a key difference that contributed to the different response seen in *Casp1*$^{-/-}$ mice after HDM administration. In addition, this does not appear to be an IL-1 effect, as IL-1 receptor (*Il1r*$^{-/-}$)–deficient mice also did not show any difference in cell infiltrates and particularly not in eosinophil counts after HDM administration in our HDM model (Fig. S6*A*). Furthermore, *AMCase-ED* mice also showed no difference to wild-type mice in airway inflammation and the production of IL-5 and IL-13 in the adjuvant-dependent i.p. sensitization OVA–Alum model, suggesting that the increased type 2 immune responses in *AMCase-ED* mice after HDM administration are highly correlated to chitin itself and the enzymatic activity of AMCase (Fig. S6 *B* and *C*).

**HDM Promotes Increased IL-33 Production in *AMCase-ED* and *Casp1*$^{-/-}$ Mice.** It is well known that HDM instructs a type 2 immune response via the release of innate pro-Th2 cytokines including TSLP, IL-25, and IL-33 (1, 3, 26). Indeed, a recent report that showed that IL-33, but not TSLP or IL-25, is central to mite and peanut allergic sensitization led us to focus on IL-33 (27). Moreover, another report showed that *IL-33*$^{-/-}$ mice exhibited a significantly diminished inflammatory cell influx into the BAL fluid after HDM administration (28). Because AMCase is secreted by both epithelial cells and macrophages (15), we performed bone marrow chimeras of WT and *AMCase-ED* mice (where *AMCase-ED* or WT bone marrow was injected into irradiated *AMCase-ED* or WT recipients) to distinguish the role of epithelial cells and macrophages. Both WT → *AMCase-ED* and *AMCase-ED* → WT chimeric mice showed greater airway inflammation compared with WT → WT mice but less infiltration compared with *ED* → *ED* mice, suggesting that both epithelial cells and macrophages contribute biologically significant amounts of AMCase (Fig. 5*A* and Fig. S7). As WT → *ED* chimeric mice showed a somewhat greater increase in total cell number and eosinophil number comparing to *ED* → WT chimeric mice, it is possible that epithelial cells may play a greater role in secreting AMCase than macrophages although we cannot exclude the possibility of the contribution of radio-resistant hematopoietic cells. As expected, control *AMCase-ED* → *AMCase-ED* mice showed a greater cell infiltrate in the BAL comparing to WT → WT chimeric mice, and again the majority of increased cells were eosinophils. Moreover, *ED* → *ED* mice secreted more IL-33 in the BAL compared to WT → WT mice, which suggests that the stronger type 2 immune responses were indeed correlated with greater release of IL-33 in the BAL (Fig. 5*B*). Both *AMCase-ED* mice and *Casp1*$^{-/-}$ mice indeed showed elevated release of IL-33 in the BAL compared to WT mice (Fig. 5 *C* and *D*). Interestingly, chitin itself promoted the release of IL-33 in

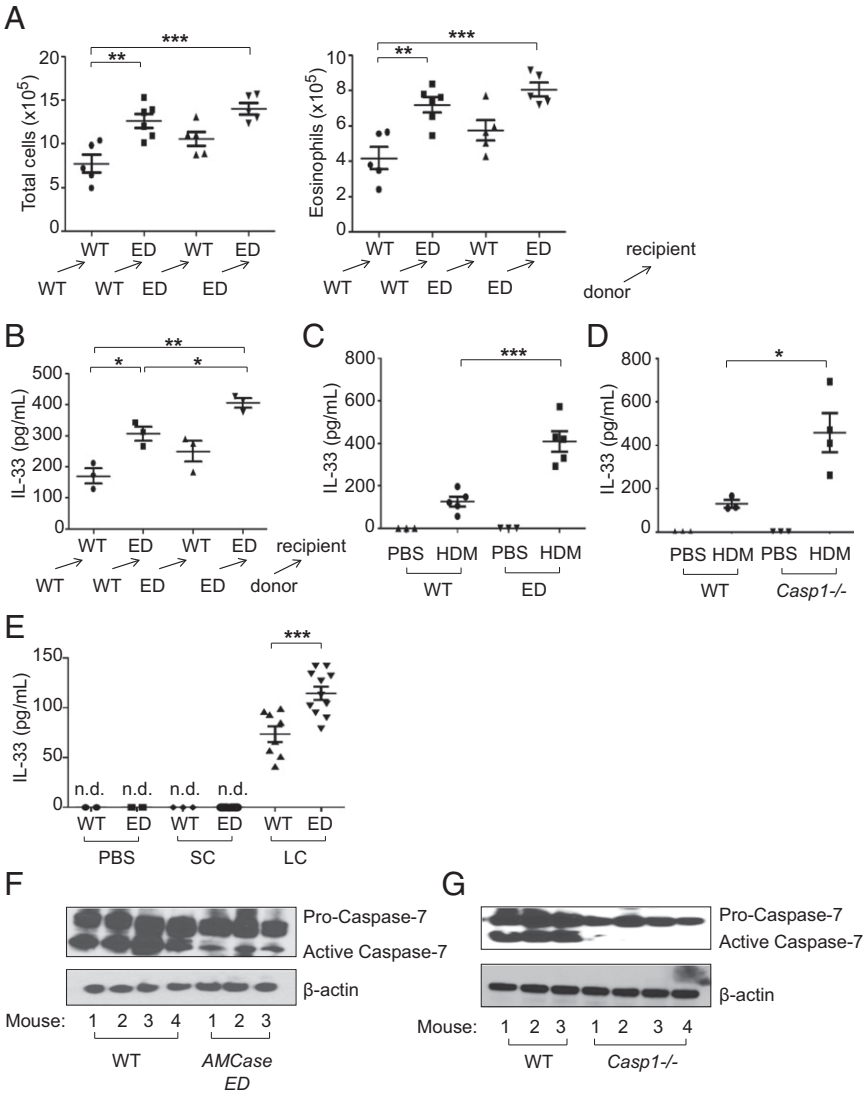


**Fig. 5.** Enhanced production of IL-33 in *AMCase-ED* mice after administration of HDM or chitin. (*A*) The number of total cells (*Left*) and eosinophils (*Right*) in the BAL of WT → WT (where WT bone marrow was injected into irradiated WT recipients), WT → *AMCase-ED*, *AMCase-ED* → WT, or *AMCase-ED* → *AMCase-ED* mice after administration of HDM. (*B*) Production of IL-33 in the BAL of WT → WT, WT → *AMCase-ED*, *AMCase-ED* → WT, or *AMCase-ED* → *AMCase-ED* mice after administration of HDM. (*C*) Production of IL-33 in the BAL of WT or *AMCase-ED* mice after administration of PBS or HDM. (*D*) Production of IL-33 in the BAL of WT or *Casp1*$^{-/-}$ mice after administration of PBS or HDM. (*E*) Production of IL-33 in the BAL of WT or *AMCase-ED* mice after administration of PBS, small chitin, or large chitin. (*F*) Immunoblot analysis of caspase-7 and β-actin in lung lysates from WT mice or *AMCase-ED* mice after administration of PBS or HDM. The number indicates the individual mouse. (*G*) Immunoblot analysis of caspase-7 and β-actin in lung lysates from WT mice or *Casp7*$^{-/-}$ mice after administration of PBS or HDM. The number indicates the individual mouse. *$P < 0.05$, **$P < 0.01$, and ***$P < 0.001$, unpaired Student's *t* test. Data were combined from at least three independent experiments. Error bars indicate the SEM.

the BAL. Although IL-33 was not detected when small chitin was administrated, copious IL-33 was released in *AMCase-ED* mice compared to WT mice upon large-chitin administration (Fig. 5*E*). These results suggest that uncleaved chitin cannot be phagocytosed into the cells and may reside outside the cells, which may promote tissue damage and thus the release of IL-33 in the lung. This in turn supports the concept that an important function of AMCase is to attenuate this response.

**Activation of Caspase-7 Is Dependent on Caspase-1.** It has been reported that full-length IL-33 is biologically active (29–31) and is processed into an inactive form by caspases such as caspase-7, activated during apoptosis (30, 32). Similarly, it is also reported that inflammasome-activated caspase-7 cleaves PARP1 to enhance the expression of a subset of NF-kappaB target genes, and, in that study, caspase-7 activation was found to be dependent on caspase-1 (33). Moreover, it was reported that caspase-7 activation by the Nlrc4 inflammasome restricts *Legionella pneumophila* infection, and again caspase-7 activation was also shown to be dependent on caspase-1 (34). We therefore hypothesized that IL-33 is cleaved into its inactive form by caspase-7, which is activated by caspase-1, which itself is activated by HDM administration. To address this model, we checked caspase-7 activation after HDM administration. Interestingly, caspase-7 activation was abrogated in the lungs of *AMCase-ED* mice (Fig. 5*F*) and almost absent from *Casp1*$^{-/-}$ mice after HDM administration (Fig. 5*G*). Moreover, we checked IL-33 cleavage in lung extracts. More cleaved IL-33 was found in WT mice than in *AMCase-ED* mice (Fig. S8). These results suggest that inefficient activation of caspase-1 or complete loss of caspase-1 in mutant mice may cause failure of caspase-7 activation, which in turn leads to prolonged exposure to active IL-33 and thus enhanced type 2 immune responses.

***Casp7*$^{-/-}$ Mice Show More Type 2 Immune Responses to Inhaled HDM.** To address the prediction that type 2 immune responses should be enhanced in the absence of caspase-7 activation, we administrated HDM intranasally into *Casp7*$^{-/-}$ mice. The cell infiltrates in BAL were significantly increased in *Casp7*$^{-/-}$ mice after HDM administration compared to WT mice, and the majority of the increased cells were eosinophils (Fig. 6*A* and Fig. S9*A*). The production of IL-5 and IL-13 from T cells from draining lymph nodes of *Casp7*$^{-/-}$ mice was also higher than in WT mice when T cells were restimulated with HDM (Fig. 6*B*). Total IgE and HDM-specific IgE levels were again higher in *Casp7*$^{-/-}$ mice (Fig. 6*C* and Fig. S9*B*), and the expression of ccl11, ear11, and muc5b was also increased in the lung of *Casp7*$^{-/-}$ mice (Fig. 6*D*). Histologic analysis showed more inflammation in *Casp7*$^{-/-}$ mice as well (Fig. 6*E*), and, finally, the secretion of IL-33 in the BAL was significantly higher in *Casp7*$^{-/-}$ mice compared to WT control mice after HDM administration (Fig. 6*F*). Taken together, all data suggest that the enhanced type 2 immune responses seen in *Casp7*$^{-/-}$ mice result from the failure to inactivate IL-33 effectively in the lung.

## Discussion

In this study, we found that the enzymatic activity of AMCase negatively regulates type 2 immune responses to allergens containing chitin. The results support the following model. The enzymatically cleaved chitin is taken up by cells through phagocytosis,

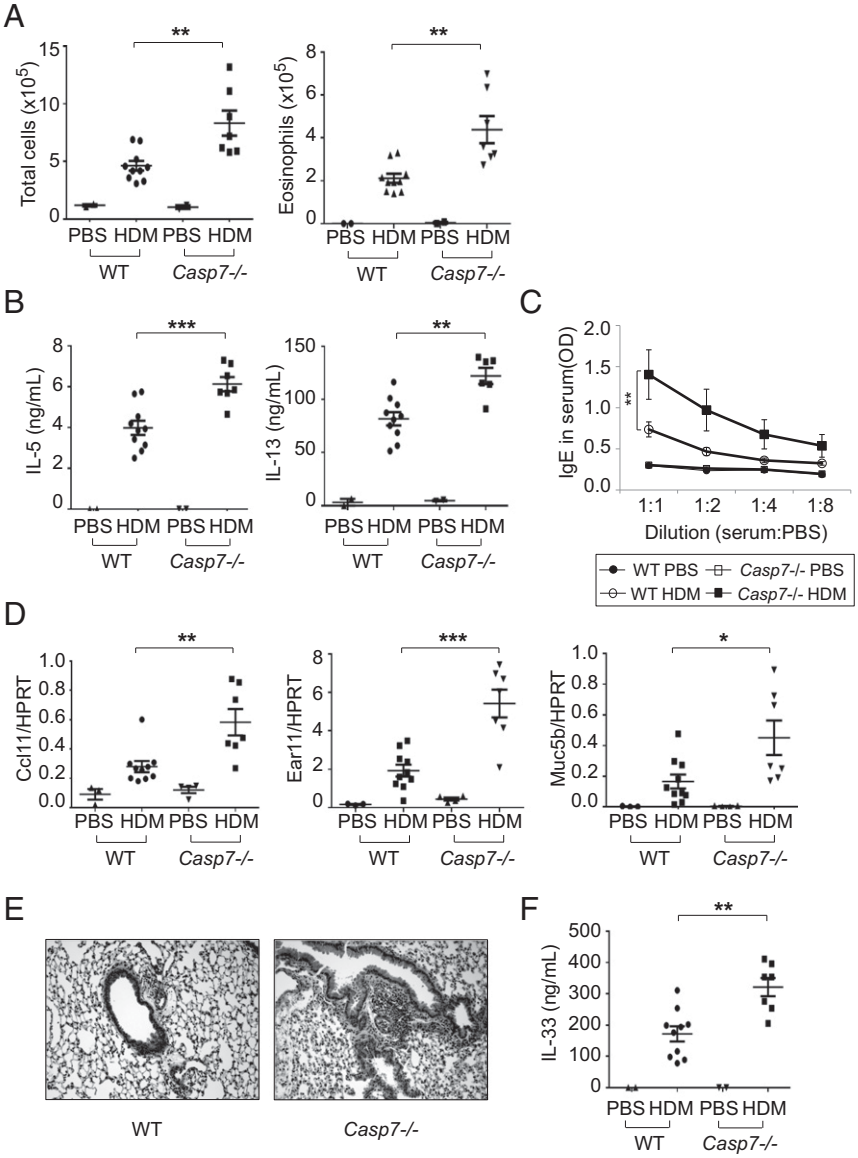


**Fig. 6.** Enhanced type 2 immune responses to inhaled HDM in *Casp7*$^{-/-}$ mice. (*A*) The number of total cells (*Left*) or eosinophils (*Right*) in the BAL of WT or *Casp7*$^{-/-}$ mice after administration of PBS or HDM. (*B*) Production of IL-5 (*Left*) and IL-13 (*Right*). The cells of lung-draining lymph nodes from WT or *Casp7*$^{-/-}$ mice after administration of PBS or HDM were restimulated in vitro with HDM and mitomycin-C–treated splenocytes for 48 h. Supernatants were collected and analyzed for IL-5 and IL-13 by ELISA. (*C*) Levels of IgE in serum of WT or *Casp7*$^{-/-}$ mice after administration of PBS or HDM. The serum was diluted with PBS sequentially and analyzed for IgE by ELISA. (*D*) Expression of ccl11, ear11, and muc5b, normalized to HPRT, in the lung of WT or *Casp7*$^{-/-}$ mice after administration of PBS or HDM. (*E*) H&E staining of lung sections of WT or *Casp7*$^{-/-}$ mice after administration of PBS or HDM (magnification: 20x). (*F*) Production of IL-33 in the BAL of WT or *Casp7*$^{-/-}$ mice after administration of PBS or HDM. $^{*}P < 0.05$, $^{**}P < 0.01$, and $^{***}P < 0.001$, unpaired Student's *t* test. Data were combined from at least three independent experiments. Error bars indicate the SEM.

which then triggers activation of caspase-1 through this well-characterized pathway (35, 36), whereas uncleaved chitin promotes the release of IL-33 probably due to mechanical damage to lung tissue. The activation of caspase-1 leads in turn to the activation of caspase-7, which inactivates IL-33, thereby resolving type 2 immune responses (Fig. S10).

In the absence of the enzymatic activity of AMCase, we found that (*i*) chitin could not be cleaved or phagocytosed; (*ii*) chitin could not activate caspase-1 and subsequently caspase-7, which (*iii*) led to prolonged exposure of active IL-33 and (*iv*) sustained type 2 immune responses.

It is interesting that chitins of different sizes have different effects both in vivo and in vitro (19, 21). It was previously reported that intranasal administration of chitin beads induced infiltration of IL-4–expressing cells in lung, but administration of chitin beads that were pretreated with recombinant AMCase failed to induce infiltration of IL-4–expressing cells in lung (11). It was also reported that mice that expressed AMCase constitutively in lung demonstrated a significant reduction of eosinophil infiltration after administration of chitin beads or fungal challenge (11, 35). These reports support our observations that enzymatically inactive *AMCase-ED* mice showed enhanced infiltration of eosinophils in lung and type 2 immune responses after administration of HDM or chitin. It is interesting that small chitin (less than 40 μm) induced IL-10 production in vitro and in vivo (21), suggesting that cleaved chitin may play an inhibitory role in inflammatory responses. However, production of IL-10 by small chitin was increased in cytochalasin D-treated macrophages, and thus this may be independent of caspase-1 and caspase-7 pathways.

The role of chitin in the immune system is very controversial (19, 21, 37, 38). One of the main reasons for this controversy is that it is difficult to extensively purify chitin (37, 38). Consequently, we cannot exclude the possibility that our chitin does not contain bioactive contaminants that might contribute to the observed immune responses. We believe, however, that many lines of evidence support our model for the role of AMCase enzymatic activity and chitin cleavage in the physiologically relevant HDM. Further investigation into the relationship between chitin and immune responses will be needed.

It has been reported that AMCase-deficient mice did not show dramatic defects after sensitization and challenge with OVA or HDM plus cockroach allergen (39). These results seem to conflict with our observations. Further work will be required to resolve this by direct comparison of the two strains. One important difference, however, is that our *AMCase-ED* mice still express AMCase protein that can bind to chitin, although its catalytic chitinase activity is defective in the lung.

We demonstrated that caspase-7 was activated following HDM treatment and that the activation of caspase-7 is defective in *Casp1*$^{-/-}$ mice as well as *AMCase-ED* mice. Caspase-7 has been suggested to be a substrate of the caspase-1 inflammasome using targeted peptidecentric proteomics (40). In addition, it was reported that caspase-7 activation after *L. pneumophila* infection was dependent on caspase-1 (34). Most recently, it was reported that caspase-7 is activated by caspase-1 after LPS stimulation although in that study the activated caspase-7 was shown to translocate to the nucleus where it played a nuclear function (33). Altogether, we therefore believe that many published reports support our finding that caspase-7 activation is dependent on caspase-1 activated during HDM administration. However, it is still unclear whether caspase-7 activation is due to cell death, an inflammatory pathway, or other effects that follow HDM administration.

Regarding the inactivation of IL-33, it was reported that the biological activity of IL-33 was suppressed through proteolysis by apoptotic caspases such as caspase-3 and caspase-7 (32). Indeed, we observed elevated IL-33 in the BAL and enhanced type 2 immune responses in *Casp7*$^{-/-}$ mice, suggesting a defect in IL-33 inactivation in the absence of caspase-7 although we cannot exclude the possibility of the role of other proteases and caspases (41–43). Considering the fact that IL-33 is a nuclear protein (31), it is possible that the activated caspase-7 that is translocated into the nucleus following activation by caspase-1 may play a role in IL-33 processing in the nucleus.

In conclusion, by using a newly generated enzymatically dead AMCase knockin mouse, we found that AMCase plays a crucial role in the control of type 2 immune responses to HDM. As a result, mice lacking the enzymatic activity of AMCase showed a greater immune response. In addition, we have elucidated the signal cascades that control type 2 immune responses upon HDM administration and how these signal cascades are misregulated in the absence of AMCase enzymatic activity. Further investigation of this pathway and its relevance to human asthma will be of interest.

## Materials and Methods

**Mice.** *AMCase-ED* mice were generated by the standard ES cell gene-targeting strategy. AMCase gene fragments were cloned from BAC clone RP23-277I1 (CHORI) containing whole mouse AMCase gene. We introduced GCC at codon 138 in exon 5 of AMCase by in vitro mutagenesis. We also introduced NruI to identify the mutant allele without any amino acid changes. A 2.5-kb short fragment and 3.0-kb fragment including a mutated region were ligated into pEasy-Flox vector. The construct was transfected into C57BL/6 as well as 129 ES cells. ES cells were cultured with G-418/Neomycin and Gancyclovir to enrich the recombinant ES cells positively and negatively. A total of 216 B6 ES colonies and 216 129 ES colonies were harvested and screened by PCR. There were two correctly targeted ES cells from the C57BL/6 and one from the 129 ES cells. All three clones were injected into C57BL/6 blastocysts generating chimeric mice. The chimeric mice were bred, and germline-transmitting knockin mice were generated. Mice use in these experiments had been backcrossed to C57BL/6Ncr more than 10 times. Genotyping PCR was performed using the following primers: F—5′-ACTGGGAGTTTGGAAGAATAG-3′ and R—5′-CTCACACAGTCCT-TGACAAGGA-3′. The generation of *Casp1*$^{-/-}$ mice and *Casp7*$^{-/-}$ mice has been reported previously (44, 45). *Il1r*$^{-/-}$ mice were obtained from Jackson Laboratories. Age-matched and sex-matched C57BL/6Ncr (National Cancer Institute Animal Production Program) mice were used as all WT controls. All animals were bred and maintained in accordance with the Yale University Institutional Animal Care and Use Committee protocols.

**Mouse Models for Allergic Airway Disease.** For administration of HDM, HDM extract and raw HDM were purchased from Greer Laboratories (*Dermatophagoides pteronyssinus*; B84). Six to 8-wk-old mice were anesthetized with methoxyflurane (Medical Developments International) and administered intranasally with PBS or 25 μg of HDM on days 0, 1, and 2. After 2 wk, the mice were injected intranasally with PBS or 5 μg of HDM on days 14, 15, 16, and 17. On day 18, the mice were killed and 2 mL of BAL fluid, blood, and lung were collected. For administration of chitin, chitin from crab shells (Sigma, C7170, batch no. 065K7026) was suspended in endotoxin-free sterile PBS (Sigma) and then sequentially passed through 100-μm, 70-μm, and 40-μm cell strainers (BD Biosciences). The fractionated chitin mixture was washed several times with PBS and with 70% ethanol and suspended in sterile PBS and then autoclaved. Fifty micrograms of chitin mixture was intranasally administered on days 0, 1, and 2. After 2 wk, 10 μg of chitin mixture was intranasally administered again on days 14, 15, 16, and 17. On day 18, the mice were killed and 2 mL of BAL fluid, blood, and lung were collected. Ovalbumin (Grade V; Sigma) administration was done as described previously (22).

**Chitinase Activity Assay.** A chitinase assay kit (Sigma, catalog # CS0908) was used and followed per manufacturer's instructions. Briefly, BAL fluids or supernatants from cell cultures are incubated with 4-nitrophenyl *N*,*N*′-diacetyl-β-D-chitobioside at 37 °C and then stopped by adding sodium carbonate solution. The absorption was measured at 405 nm.

**RNA Analysis.** Total RNA from lung tissue was purified with TRIzol reagent (Invitrogen) and was reverse-transcribed to cDNA with SuperScript II reverse transcriptase (Invitrogen). The expression of individual genes was measured using Taqman probes (Applied Biosystem) in a 7500 Fast Real Time PCR System (Applied Biosystem).

**Dot Blotting, ELISA, and Western Analysis.** Dot blotting for chitin detection was performed as described previously (46). Antibody pairs for ELISA were purchased from R&D Systems (IL-1β and IL-33), BD Pharmingen (IL-5, IL-13, and IgE), or eBioscience (TNFα). Antibodies for Western blotting were purchased from Santa Cruz Biotechnology (caspase-1; clone M-20), Alexis Biochemicals (IL-33; 210–933), or Cell Signaling (caspase-7; #9492). ELISA and Western blotting were performed as described previously (22).

**Limulus Test.** The limulus test for endotoxin detection was performed using Limulus Amebocyte Lysate QCL-1000 (Lonza, catalog # 50–647) per manufacturer's instructions.

**T-Cell Restimulation.** T-cell restimulation for measuring IL-5 and IL-13 was performed as described previously (22). Briefly, T cells from lung-draining lymph nodes were collected from WT and *AMCase-ED*, *Casp1*$^{-/-}$, or *Casp7*$^{-/-}$ mice. Cells were restimulated in vitro with or without HDM or ovalbumin and mitomycin-C (Sigma)–treated splenocytes for 48 h. Supernatants were analyzed for IL-5 or IL-13.

**Histological Analysis.** Formalin-fixed sections of lung were prepared and stained. Hematoxylin and eosin (H&E) staining was done in the Research Histology Laboratory of the Department of Pathology at Yale School of Medicine.

**Phagocytosis Assay and Flow Cytometry.** Chitin was labeled with FITC (Thermo Scientific) per manufacturer's instructions. Thioglycollate-elicited peritoneal macrophages were prepared as described previously (22). The cells were treated with FITC-labeled chitin or FITC-conjugated latex beads (Cayman Chemical, catalog # 400291) with or without bisdionin F (Calbiochem, catalog # 112252), and then flow cytometry was performed.

**Mixed Bone Marrow Chimera.** Adoptive transfer of bone marrow was performed as described previously (47). Briefly, bone marrow cells were collected and injected retro-orbitally into sublethally irradiated 5- to 6-wk-old mice. The recipients were analyzed 10–12 wk after transplantation for complete chimerism.

**Statistical Analysis.** An unpaired Student's *t* test was performed for statistical analysis for all studies using GraphPad Prism software. $P < 0.05$ was considered statistically significant.

**ACKNOWLEDGMENTS.** We thank J. Alderman and C. Lieber for technical assistance and discussions. This work was supported in part by the Howard Hughes Medical Institute (R.A.F. and L.K.K.) and by the National Heart, Lung and Blood Institute (Grant 1 RC1 HL100738 to R.A.F.).

1. Gregory LG, Lloyd CM (2011) Orchestrating house dust mite-associated allergy in the lung. *Trends Immunol* 32(9):402–411.
2. Lambrecht BN, Hammad H (2012) The airway epithelium in asthma. *Nat Med* 18(5): 684–692.
3. Hammad H, Lambrecht BN (2008) Dendritic cells and epithelial cells: Linking innate and adaptive immunity in asthma. *Nat Rev Immunol* 8(3):193–204.
4. Palm NW, Rosenstein RK, Medzhitov R (2012) Allergic host defences. *Nature* 484(7395):465–472.
5. Pulendran B, Artis D (2012) New paradigms in type 2 immunity. *Science* 337(6093): 431–435.
6. Lee CG, Da Silva CA, Lee JY, Hartl D, Elias JA (2008) Chitin regulation of immune responses: An old molecule with new roles. *Curr Opin Immunol* 20(6):684–689.
7. Lee CG, et al. (2011) Role of chitin and chitinase/chitinase-like proteins in inflammation, tissue remodeling, and injury. *Annu Rev Physiol* 73:479–501.
8. Shibata Y, Metzger WJ, Myrvik QN (1997) Chitin particle-induced cell-mediated immunity is inhibited by soluble mannan: Mannose receptor-mediated phagocytosis initiates IL-12 production. *J Immunol* 159(5):2462–2467.
9. Shibata Y, Foster LA, Bradfield JF, Myrvik QN (2000) Oral administration of chitin down-regulates serum IgE levels and lung eosinophilia in the allergic mouse. *J Immunol* 164(3):1314–1321.
10. Strong P, Clark H, Reid K (2002) Intranasal application of chitin microparticles down-regulates symptoms of allergic hypersensitivity to Dermatophagoides pteronyssinus and Aspergillus fumigatus in murine models of allergy. *Clin Exp Allergy* 32(12): 1794–1800.
11. Reese TA, et al. (2007) Chitin induces accumulation in tissue of innate immune cells associated with allergy. *Nature* 447(7140):92–96.
12. Sandler NG, Mentink-Kane MM, Cheever AW, Wynn TA (2003) Global gene expression profiles during acute pathogen-induced pulmonary inflammation reveal divergent roles for Th1 and Th2 responses in tissue repair. *J Immunol* 171(7):3655–3667.
13. Xu Y, et al. (2003) Transcriptional adaptation to cystic fibrosis transmembrane conductance regulator deficiency. *J Biol Chem* 278(9):7674–7682.
14. Boot RG, et al. (2005) Marked differences in tissue-specific expression of chitinases in mouse and man. *J Histochem Cytochem* 53(10):1283–1292.
15. Zhu Z, et al. (2004) Acidic mammalian chitinase in asthmatic Th2 inflammation and IL-13 pathway activation. *Science* 304(5677):1678–1682.
16. Qureshi AM, Hannigan A, Campbell D, Nixon C, Wilson JB (2011) Chitinase-like proteins are autoantigens in a model of inflammation-promoted incipient neoplasia. *Genes Cancer* 2(1):74–87.
17. Lee CG, et al. (2009) Role of breast regression protein 39 (BRP-39)/chitinase 3-like-1 in Th2 and IL-13-induced tissue responses and apoptosis. *J Exp Med* 206(5):1149–1166.
18. Hartl D, et al. (2009) Acidic mammalian chitinase regulates epithelial cell apoptosis via a chitinolytic-independent mechanism. *J Immunol* 182(8):5098–5106.
19. Bueter CL, et al. (2011) Chitosan but not chitin activates the inflammasome by a mechanism dependent upon phagocytosis. *J Biol Chem* 286(41):35447–35455.
20. Bueter CL, Specht CA, Levitz SM (2013) Innate sensing of chitin and chitosan. *PLoS Pathog* 9(1):e1003080.
21. Da Silva CA, et al. (2009) Chitin is a size-dependent regulator of macrophage TNF and IL-10 production. *J Immunol* 182(6):3573–3582.
22. Eisenbarth SC, Colegio OR, O'Connor W, Sutterwala FS, Flavell RA (2008) Crucial role for the Nalp3 inflammasome in the immunostimulatory properties of aluminium adjuvants. *Nature* 453(7198):1122–1126.
23. Konno S, et al. (1996) Cytokine concentrations in sputum of asthmatic patients. *Int Arch Allergy Immunol* 109(1):73–78.
24. Thomas SS, Chhabra SK (2003) A study on the serum levels of interleukin-1beta in bronchial asthma. *J Indian Med Assoc* 101(5):282, 284, 286 passim.
25. Birrell MA, Eltom S (2011) The role of the NLRP3 inflammasome in the pathogenesis of airway disease. *Pharmacol Ther* 130(3):364–370.
26. Hammad H, et al. (2009) House dust mite allergen induces asthma via Toll-like receptor 4 triggering of airway structural cells. *Nat Med* 15(4):410–416.
27. Chu DK, et al. (2013) IL-33, but not thymic stromal lymphopoietin or IL-25, is central to mite and peanut allergic sensitization. *J Allergy Clin Immunol* 131(1):187–200; e181–e188.
28. Oboki K, et al. (2010) IL-33 is a crucial amplifier of innate rather than acquired immunity. *Proc Natl Acad Sci USA* 107(43):18581–18586.
29. Talabot-Ayer D, Lamacchia C, Gabay C, Palmer G (2009) Interleukin-33 is biologically active independently of caspase-1 cleavage. *J Biol Chem* 284(29):19420–19426.
30. Liew FY, Pitman NI, McInnes IB (2010) Disease-associated functions of IL-33: The new kid in the IL-1 family. *Nat Rev Immunol* 10(2):103–110.
31. Palmer G, Gabay C (2011) Interleukin-33 biology with potential insights into human diseases. *Nat Rev Rheumatol* 7(6):321–329.
32. Lüthi AU, et al. (2009) Suppression of interleukin-33 bioactivity through proteolysis by apoptotic caspases. *Immunity* 31(1):84–98.
33. Erener S, et al. (2012) Inflammasome-activated caspase 7 cleaves PARP1 to enhance the expression of a subset of NF-κB target genes. *Mol Cell* 46(2):200–211.
34. Akhter A, et al. (2009) Caspase-7 activation by the Nlrc4/Ipaf inflammasome restricts Legionella pneumophila infection. *PLoS Pathog* 5(4):e1000361.
35. Jin C, Flavell RA (2010) Molecular mechanism of NLRP3 inflammasome activation. *J Clin Immunol* 30(5):628–631.
36. Latz E, Xiao TS, Stutz A (2013) Activation and regulation of the inflammasomes. *Nat Rev Immunol* 13(6):397–411.
37. Wagener J, et al. (2014) Fungal chitin dampens inflammation through IL-10 induction mediated by NOD2 and TLR9 activation. *PLoS Pathog* 10(4):e1004050.
38. Alvarez FJ (2014) The effect of chitin size, shape, source and purification method on immune recognition. *Molecules* 19(4):4433–4451.
39. Fitz LJ, et al. (2012) Acidic mammalian chitinase is not a critical target for allergic airway disease. *Am J Respir Cell Mol Biol* 46(1):71–79.
40. Lamkanfi M, et al. (2008) Targeted peptidecentric proteomics reveals caspase-7 as a substrate of the caspase-1 inflammasomes. *Mol Cell Proteomics* 7(12):2350–2363.
41. Hayakawa M, et al. (2009) Mature interleukin-33 is produced by calpain-mediated cleavage in vivo. *Biochem Biophys Res Commun* 387(1):218–222.
42. Lefrançais E, et al. (2012) IL-33 is processed into mature bioactive forms by neutrophil elastase and cathepsin G. *Proc Natl Acad Sci USA* 109(5):1673–1678.
43. Lefrançais E, Cayrol C (2012) Mechanisms of IL-33 processing and secretion: Differences and similarities between IL-1 family members. *Eur Cytokine Netw* 23(4):120–127.
44. Sutterwala FS, et al. (2006) Critical role for NALP3/CIAS1/Cryopyrin in innate and adaptive immunity through its regulation of caspase-1. *Immunity* 24(3):317–327.
45. Lakhani SA, et al. (2006) Caspases 3 and 7: Key mediators of mitochondrial events of apoptosis. *Science* 311(5762):847–851.
46. Van Dyken SJ, et al. (2011) Fungal chitin from asthma-associated home environments induces eosinophilic lung infiltration. *J Immunol* 187(5):2261–2267.
47. Taki S, Meiering M, Rajewsky K (1993) Targeted insertion of a variable region gene into the immunoglobulin heavy chain locus. *Science* 262(5137):1268–1271.

# Supporting Information

Kim et al. 10.1073/pnas.1507393112

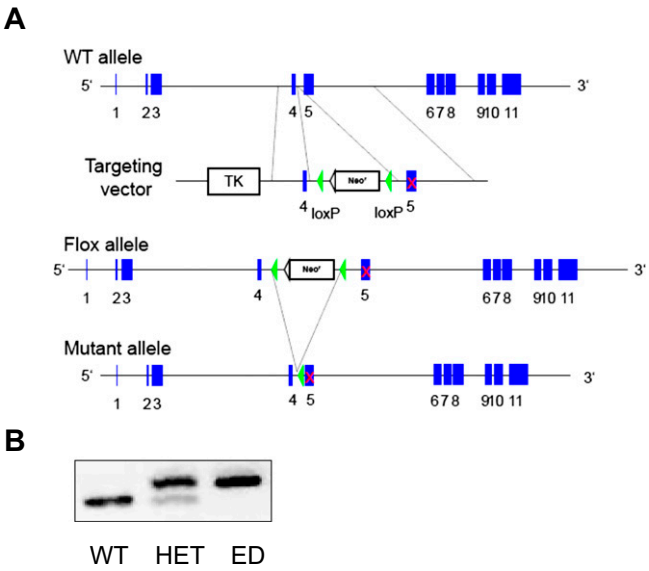


**Fig. S1.** (*A*) Targeting strategy of *AMCase-ED* mice. (*B*) Genotyping PCR. WT allele gives a 120-bp fragment, whereas *AMCase-ED* allele gives a 150-bp fragment. The primer sequences are listed in *Materials and Methods*.

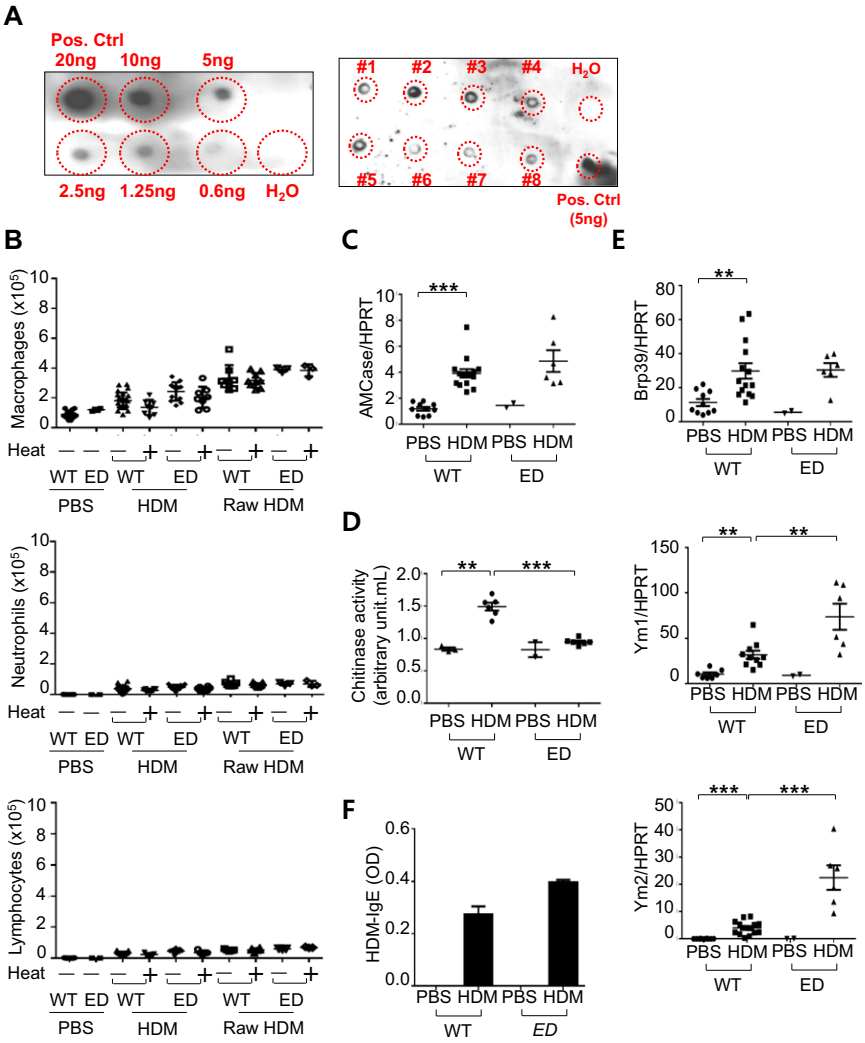


**Fig. S2.** Detection of chitin in HDM. (*A*) Dot blotting for chitin. A different dose of chitin is used as positive control (*Left*) and eight different batches of HDM are used (*Right*). A detail about chitin preparation is described in *Materials and Methods*. (*B*) The number of macrophages (*Top*), neutrophils (*Middle*), or lymphocytes (*Bottom*) in the BAL of WT or *AMCase-ED* mice after administration of PBS, HDM, or raw HDM with (+) or without (–) pretreatment at 95 °C for 10 min. (*C*) Expression of AMCase, normalized to HPRT, in the lung of WT or *AMCase-ED* mice after administration of PBS or HDM. (*D*) Chitinase activity in the BAL of WT mice or *AMCase-ED* mice after administration of PBS or HDM. (*E*) Expression of Brp39 (*Top*), Ym1 (*Middle*), and Ym2 (*Bottom*), normalized to HPRT, in the lung of WT or *AMCase-ED* mice after administration of PBS or HDM. (*F*) Levels of HDM-specific IgE in serum of WT or *AMCase-ED* mice after administration of PBS or HDM. $^{**}P < 0.01$ and $^{***}P < 0.001$, unpaired Student's *t* test. Data were combined from at least four independent experiments. Error bars indicate the SEM.

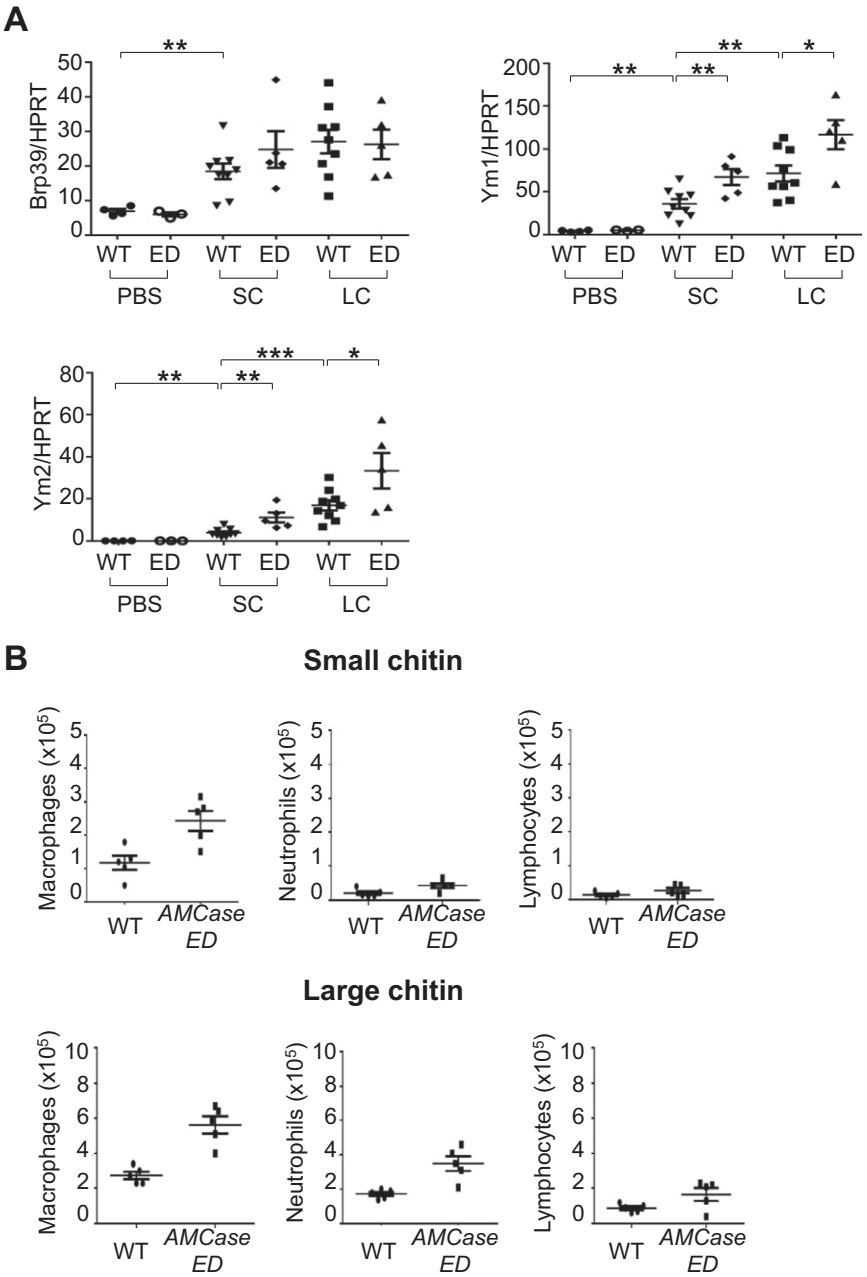


**Fig. S3.** Expression of CLPs after administration of small-chitin or large-chitin fragments. (*A*) Expression of Brp39, Ym1, and Ym2, normalized to HPRT, in the lung of WT or *AMCase-ED* mice after administration of PBS, small-chitin, or large-chitin fragments. (*B*) The number of macrophages (*Left*), neutrophils (*Middle*), or lymphocytes (*Right*) in the BAL of WT mice after administration of small-chitin (*Top*) and large-chitin (*Bottom*) fragments. $*P < 0.05$, $**P < 0.01$, and $***P < 0.001$, unpaired Student's *t* test. Data were combined from at least three independent experiments. Error bars indicate the SEM.

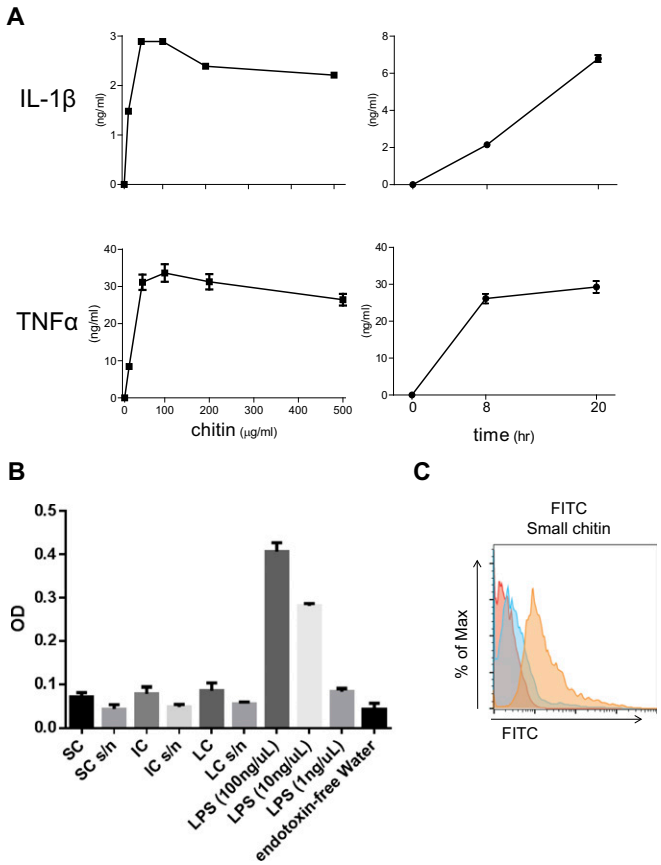


**Fig. S4.** Production of IL-1β or TNFα after chitin treatment. (*A*) Production of IL-1β or TNFα in the supernatants of LPS-primed peritoneal macrophages from WT mice after treatment with the mixture of chitin. (*B*) The limulus test was performed using small-, intermediate-, and large-chitin fragments and their supernatants. LPS and endotoxin-free water were used as controls. "s/n" indicates the supernatants. (*C*) Histograms of fluorescence distribution of the mixture of peritoneal macrophages from WT mice. Red represents WT cells with DMSO, orange represents the cells with FITC small chitin, and blue represents the cells with FITC small chitin and AMCase inhibitor, biodionin F treatment. Error bars indicate the SD.

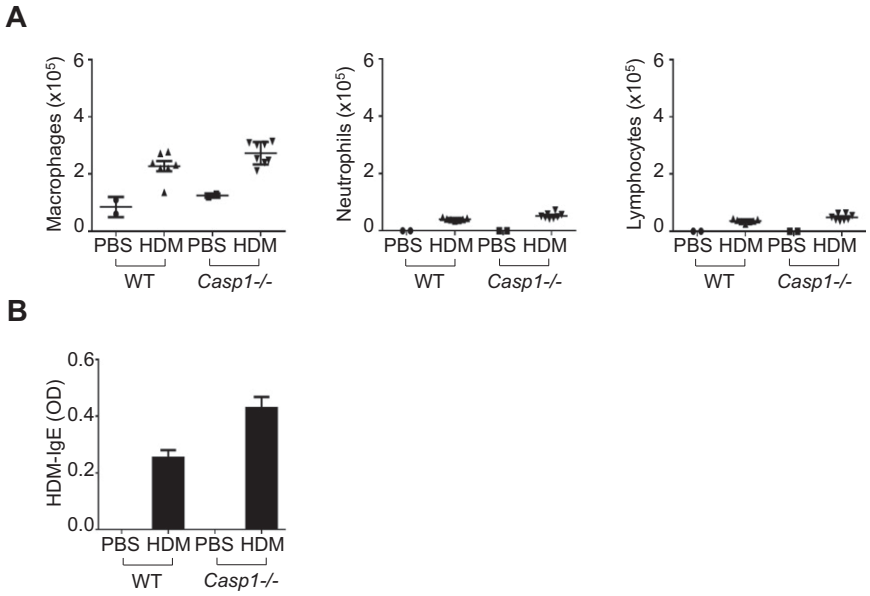


**Fig. S5.** WT and *Casp1*$^{-/-}$ mice after administration of HDM. (*A*) The number of macrophages (left), neutrophils (middle) or lymphocytes (right) in the BAL of WT or *Casp1*$^{-/-}$ mice after administration of PBS or HDM. (*B*) Levels of HDM specific IgE in serum of WT or *Casp1*$^{-/-}$ mice after administration of PBS or HDM. Data were combined from at least three independent experiments. Error bars indicate the SEM.

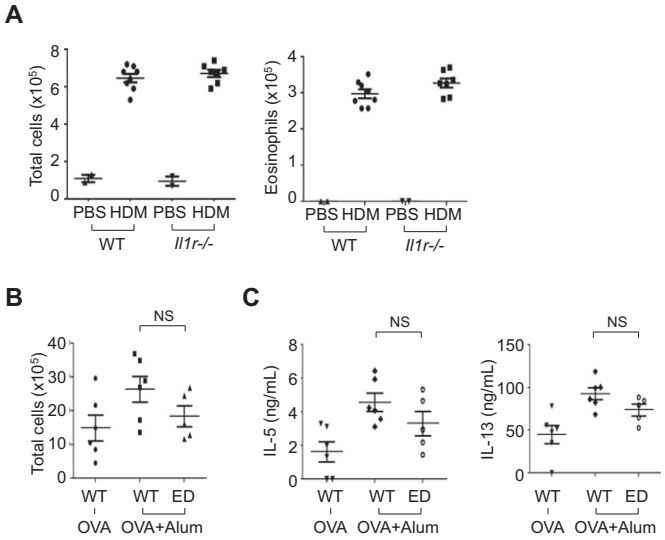


**Fig. S6.** WT and *Il1r*$^{-/-}$ mice after administration of HDM. (*A*) The number of total cells (*Left*) or eosinophils (*Right*) in the BAL of WT or *Il1r*$^{-/-}$ mice after administration of PBS or HDM. (*B*) The number of total cells in the BAL of WT or *AMCase-ED* mice after administration of OVA. (*C*) Production of IL-5 (*Left*) and IL-13 (*Right*). Unpaired Student's *t* test was performed. Error bars indicate the SEM.

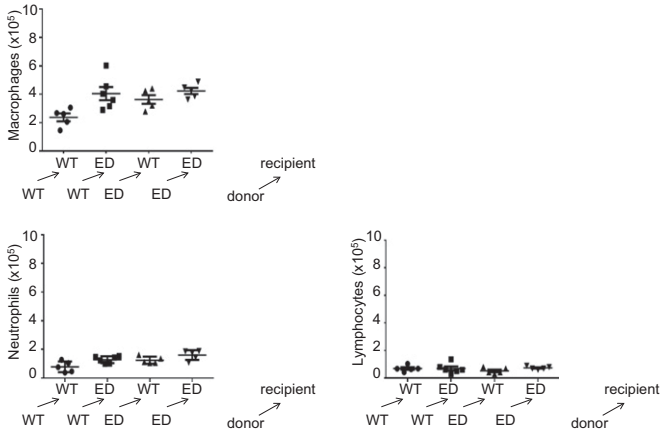


**Fig. S7.** The number of macrophages, neutrophils, or lymphocytes in the BAL of WT → WT (where WT bone marrow was injected into irradiated WT recipients), WT → *AMCase-ED*, *AMCase-ED* → WT, or *AMCase-ED* → *AMCase-ED* mice after administration of HDM. Error bars indicate the SEM.

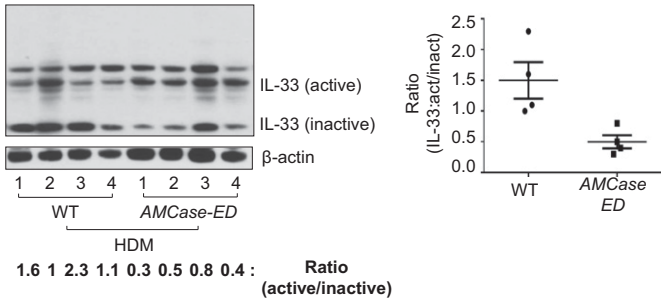


**Fig. S8.** IL-33 processing in the lung in WT or *AMCase-ED* mice after administration of HDM. Immunoblot analysis of IL-33 and β-actin in lung lysates from WT mice or *AMCase-ED* mice after administration of HDM. The number (immediately below the immunoblot analysis) indicates the individual mouse. The bolder numbers are the ratios, calculated by active IL-33 density divided by inactive IL-33 density. The density is measured using ImageJ (NIH). The ratio from each individual mouse was plotted (*Right*). Error bars indicate the SEM.

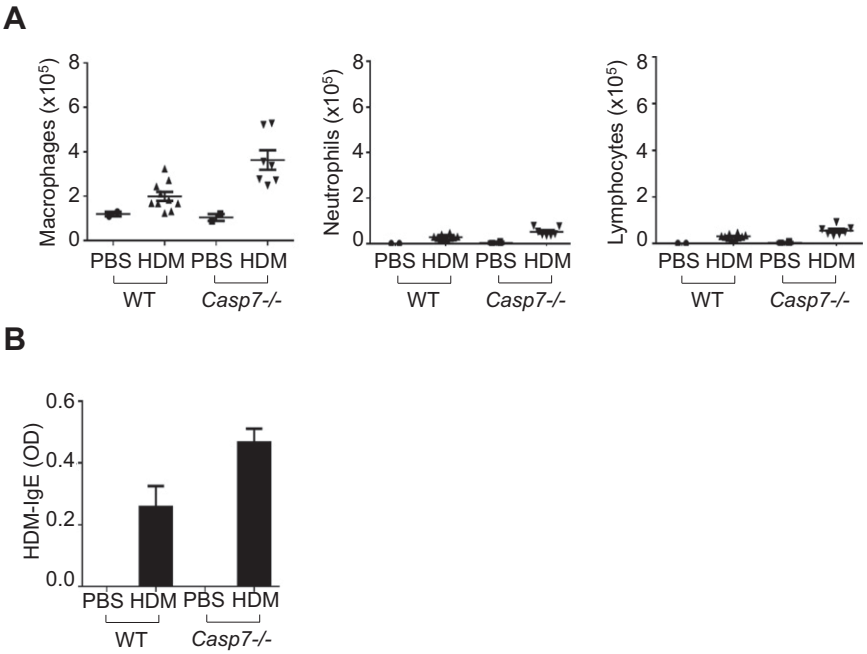


**Fig. S9.** WT and *Casp7*$^{-/-}$ mice after administration of HDM. (*A*) The number of macrophages (*Left*), neutrophils (*Middle*) or lymphocytes (*Right*) in the BAL of WT or *Casp7*$^{-/-}$ mice after administration of PBS or HDM. (*B*) Levels of HDM-specific IgE in serum of WT or *Casp7*$^{-/-}$ mice after administration of PBS or HDM. Data were combined from at least three independent experiments. Error bars indicate the SEM.

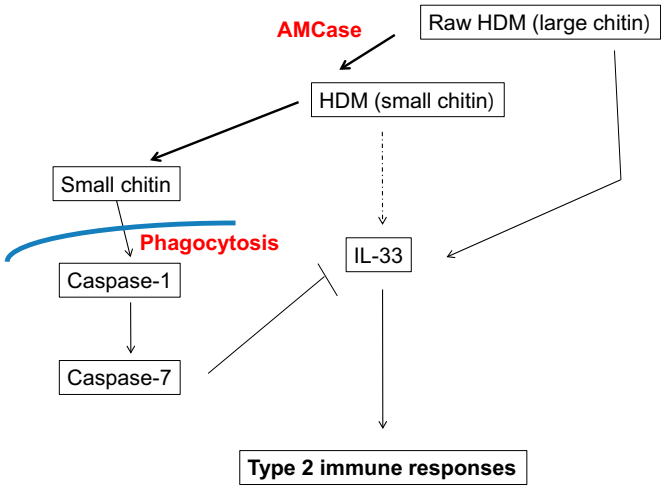


**Fig. S10.** Proposed model.